International Journal of Scientific Engineering and Research (IJSER)
ISSN (Online): 2347-3878
Impact Factor (2018): 5.426

Structural Analysis of Guyed Tower Considering a Tow Models

M. Naguib [1], A. A. Ghaleb[2], A.I. Elmetwally[3]

[1]Mohammed Naguib Mohammed Abou El-Saad, Professor of Theory of Structures,
Structural Engineering Department, Faculty of Engineering, Mansoura University, Egypt

[2]Ahmed Amin Ghaleb, Associate Professor of Concrete Structures
Structural Engineering Department, Faculty of Engineering, Mansoura University, Egypt

[3]Ahmed Ibrahim Elmetwally Elmetwally Said, Teaching Assistant of Structural Analysis and Mechanics,
Structural Engineering Department, Faculty of Engineering, Mansoura University, Egypt

Abstract: ***The key objective of the present work is to study the parameters affecting the static behavior of guyed towers. These towers consist of shafter vertical shaft with three or four legs and supported by three or four cables along its height at one level or more. The authors take into account a two different mathematical models. One of both models is modeled the shaft as line beam element with equivalent section, and other is a three-dimension flexure element as vertical legs with horizontal and diagonal lacing. This study is carried out for triangular and square guyed tower with deferent lacing systems. The spacing between shaft legs and number of levels of cables along the tower height under various velocities of wind and deferent values of initial tension in cables are taken into consideration of analyses. The obtained results are tabulated and drawn in many tables and graphs respectively. These tables explain the percentage variation of difference between deformations for the two mathematical models for all study parameters.***

Keywords: Tension structure, Cables, Guyed tower, Preliminary analysis, Different statical system

1. Introduction

During recent years a lot advanced investigations of civil engineering structures have mainly been carried out in the field of slender, relatively light and flexible structures. These investigations have been carried out for many structures such as cable and cable stayed roofs, suspension and cable stayed bridges, membranes, pneumatic structures, towers and guyed shafts.

The improvement of radio and TV administrations has brought about an interest for extremely tall structures to carry the radiating antennae· A basically monetary path for doing this is by methods of slender shafts supported at intermediate levels by flexible steel cables. All the more as of late, guyed tower are used for some different purposes, for example communications industry, wind mills, transmission of phone signals by aerials over long separation, for supporting collectors in sun powered vitality applications, and for supporting tall chimney and off-shore oil operations.

Towers may be constructed of steel, aluminum or concrete and may be free standing or guyed. Guyed shafts consist of a vertical continuous central shaft laterally supported at several levels along its height by sets of inclined pre-tensioned guys. Generally, the number of levels increases with the shaft height. The central shaft is also often referred to as the tower or the shaft. Such shafts often have flexible cantilever at the tops. The shaft itself is often a triangular lattice structure, although square lattice or cylindrical structures are also used. The individual members may be designed from tubular or angular steel sections. The joints may be riveted, bolted or welded.

The shafts are usually pined or fixed at the base. The other components of guyed shafts are the foundations, accessories of the structure, and the equipment.

The present trend in guyed shaft construction is toward higher, more complex configurations with more peculiar stiffness requirements.

The guy ropes may be of various sizes and placed at arbitrary intervals along the height of the tower for shafts with triangular or square section respectively. Typically, the guys will be steel strands and often with several guys connected to a common ground connection. Guys need not be connected to the ground at the same elevation, and each guy is usually pre-stressed to some percentage of the ultimate cable strength. For more clarification the European standards EN 1993-3-1:2006 0 already give some information about the shafts structure definition and guidelines for internal forces and moments determination.

The essential loads on towers are due to the dead weight of the structural members, the weight of supported equipment, insulators, any other associated apparatus, wind , ice loads and earthquake. Beside the ice load and earthquake, wind load remains the main factor affecting the stability of the shaft structure [2].

The loads due to wind are incredibly influenced by the shape of the tower and, in the case of noncircular trussed towers, by the orientation of the tower to the direction of the wind, the ratio of the solid area to the total enclosed area of a vertical face and the cross-sectional shape of the individual members of the tower. The ice load is doubly essential

because it increases both the area exposed to wind and the vertical load. The most difficult problems in the design of guyed towers is the assessment of the effect of turbulent wind forces on the design quantities, plus maximum guy tensions and axial loads.

Structural analyses and experimental tests were investigated in the past [3-13]. Baseos et al. [3] depict some critical aspects of the analyses performed during the 38 m high steel tower design resulting from the static, seismic and stability analyses of the steel tower prototype. Full scale field measurements [4] are carried out on a 50 m tall guyed lattice shaft located on the east coast of India near Kalpakkam. Wind load modeling and structural response of the removable guyed shaft for mobile phone networks are presented in [5]. Experimental tests were performed in order to evaluate the forces and aerodynamic coefficients on a typical cable-stayed shaft used for removable base stations. The results were obtained using the wind tunnel facility.

In Egypt, and due to environmental conditions, the effect of ice is not important in the design towers. Also, the effect of temperature fluctuations is not usually severe as any contraction or expansions of the cables are balanced by a similar behavior of the tower. Finally, we can conclude that in Egypt in addition to the self-weight of the structure and the forces set up by the· tensions in the guys the wind loads are preponderant part of the total load. [14].

2. Modeling considerations

This section will address the issue of modeling of the shaft and cables of guyed towers. A few techniques are utilized by modeling both the shaft and the cables. They vary in the level of accuracy they can provide, as well as in the expense related with their utilization. The selection by the designer of one model versus another should be based on the available resources and on the particular design stage. The most common alternatives for modeling the shaft and guys and their corresponding virtues and handicaps are presented.

2.1. Modeling of the shaft

The simplest way to model the shaft is by using an equivalent beam with equivalent sectional properties These expressions neglect the contributions of both the horizontal and diagonal members of the shaft to the axial and bending stiffness of the equivalent beam [15]. The exact way to model the shaft is considering the shaft as three-dimension flexure element. A Comparison between obtained results taken into account many study parameters are proposed

2.2. Modeling of the guys

The modeling of the guys is more complex than that of the shaft due to the inherent nonlinearity of cable structures. The behavior of cables is presented in detail in [15-20], where interested readers can be referred to for more information. For example, a novel approach in which three guys connected to the shaft at a given level are substituted by a spring was proposed in[15]. The approach introduced in [16],based on the concepts of force equilibrium, deformation compatibility, and linear elastic material behavior, was followed. Salehi Ahmad Abad et al. [19] proposed a discrete model of cable subjected to general loads.

In this paper the author models the guys as cable element using in sap2000.

3. Model Characteristics and Parametric Studies

3.1. Configuration of tower shaft and cables

The study is carried out taken into consideration the followings: both triangular and square guyed tower having a height of 44m with one and two level of cables as shown in Figs (1), (2), (3) and (4).

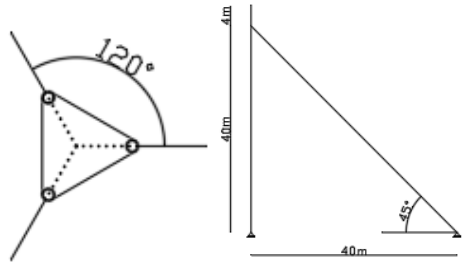

Shaft cross section tower heightand cable desistance

Figure 1: Triangular guyed tower with one cable level

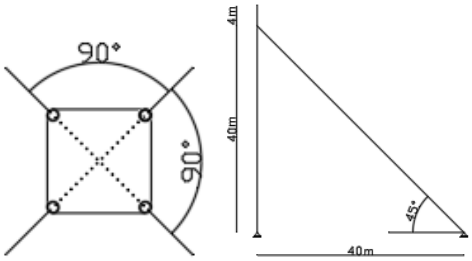

Shaft cross section tower height and cable desistance

Figure 2: Square guyed tower with one cable level

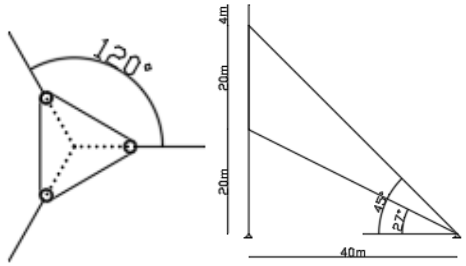

Shaft cross section tower height and cable desistance

Figure 3: Triangular guyed tower with two cable level

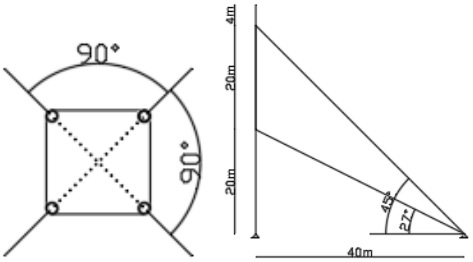

Shaft cross section tower height and cable desistance

Figure 4: Square guyed tower with two cable level.

3.2. Shaft cross section

The both cross sections of triangular and square towers with their main structural components are shown in Fig (5).

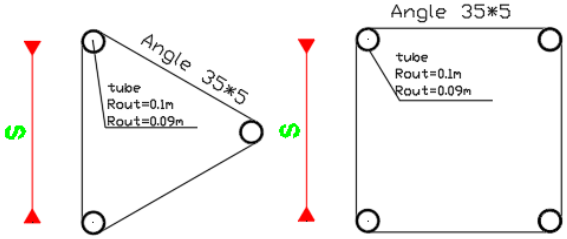

Triangular cross section Square cross section

Figure 5: Towers cross sections

3.3. System of shaft lacing

Three types of lacing system for tower shaft are shown in Fig (6).

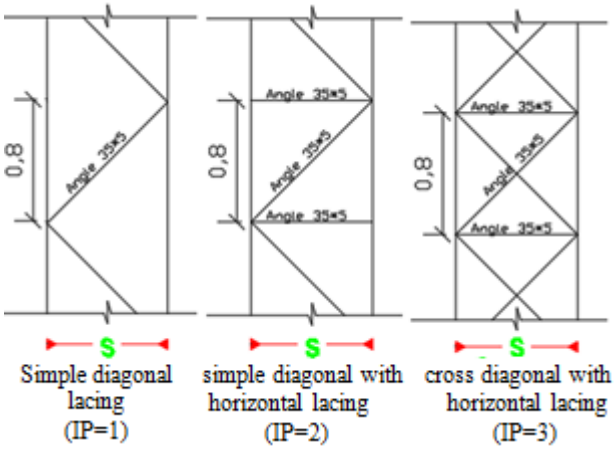

Figure 6: Towers lacing systems

3.4. Shaft dimensions

Four spacing between legs (from experience verified) are considered (0.6m, 0.8m, 1.0m and1.2m)

3.5. Initial tension in cables

The initial tension in cables is taken as (10% and 20% of breaking load)

3.6. Wind speed at 10m (U (10)).

The wind speed on the tower varies as given. U (10) equal (10m/s,20m/s,30m/s,40m/s,50m/s and 60m/s))

4. The properties of towers sections

4.1. The properties of shaft

Table 1: Properties of shaft

Section	Main leg (tube)	Diagonal Lacing (angle)	Horizontal Lacing (angle)
Cross Section Area (A) cm2	14.92	3.28	3.28
Moment of inertia about x-axis (Ix) cm4	168.8	3.56	3.56
Moment of inertia about x-axis (Iy) cm4	168.8	3.56	3.56
Polar moment of inertia (IP) cm4	337.6	7.12	7.12
Modules of elasticity, E (N/Cm2)	2.1E+11		

4.2. The properties of shaft for both cross sections with referred to Fig (5)

These properties are tabulated in both the following tables for triangular and square towers.

Table 2: Properties of sections for triangular tower

Model	Triangular tower			
Space(s)m	0.6	0.8	1	1.2
Cross Section Area (A) cm2	44.76	44.77	44.768	44.768
Moment of inertia about x-axis (Ix) cm4	27370	48260	75120	107950
Moment of inertia about x-axis (Iy) cm4	27370	48260	75120	107950
Polar moment of inertia (IP) cm4	54740	96520	150240	215900
modules of elasticity, E (N/Cm2)	2.1E+11			

Table 3: Properties of sections for square tower

Model	Square tower			
Space(s)m	0.6	0.8	1	1.2
Cross Section Area (A) cm2	59.69	59.69	59.69	59.69
Moment of inertia about x-axis (Ix) cm4	54400	96180	149900	215560
Moment of inertia about x-axis (Iy) cm4	54400	96180	149900	215560
Polar moment of inertia (IP) cm4	108800	192360	299800	431120
modules of elasticity, E (N/Cm2)	2.1E+11			

4.3. The cables properties

Table 4: Properties of cables

Section	cable
Cross Section Area (A) cm2	14
Modules of elasticity, E (N/Cm2)	1.65E+11
Pretention force (N)	12517 & 25034
Weight per unite length (N/m)	114

5. Types of loads

Three types of loads are considered as follows:

5.1. Dead load

Owen weight of structural elements

5.2. Initial tension in cables

10% and 20% of breaking load

5.3. Wind loads

The wind load is considered as equivalent wind forces acting at cables nodes and shaft joints. this equivalent wind forces are calculated as follows:

The static wind forces acting at cables nodes and shaft joints were calculated in accordance with "the recommendation for the design and analysis of guyed shafts" by IASS [22].

The increasing of horizontal wind speed with height above the ground can be described by "logarithmic law" that is derived not only from empirical data, but also from

theoretical considerations [23].

$$U(h)= 2.5u_* \ln(h/z_o) \quad (1)$$

Where:
U(h) = the wind speed at height h (m)
z_o = the roughness length, for which the values depended on the type of the ground.
h = the height above the ground.
u_* = the so-called "friction velocity" which can be found as soon as the value z_o and the velocity U(10) at height 10 m above the ground are given.

The magnitude of the wind force, W_d , in the main wind direction above the ground is given in ref. [16]by:

$$W_d= 0.5\,\rho\, R_d\, (U(h))^2 \quad (2)$$

Where
ρ = the air density (for normal condition ρ =1.25 N/m^3)
R_d = the wind resistance in the direction of the wind.

Where
R_d is calculated separately for the guys and shaft as follows:

a) Calculation of R_d for the Guys:
The wind resistance in the direction of the wind for any linear component may be taken as:

$$R_d= C_D\, A_e \sin^3\Psi \quad (3)$$

C_D = the normal drag coefficient appropriate to the element under consideration and varies with Reynolds number R_e as shown in Fig .7.

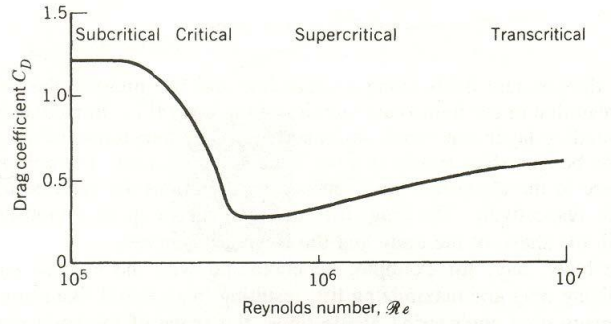

Figure 7: variation of Drag coefficient C_D with Reynolds number R_e

A_e = the area exposed to wind of the component = D*L where (D diameter of cable and L length of the element)
Ψ = the angle of wind incidence to the longitudinal axis of any linear component

$$\Psi = \cos^{-1}(\text{Cos}\,\alpha\,\text{Cos}\,\theta) \quad (4)$$

where:
α = angle of inclination of cable with horizontal plan, and
θ = angle between the plane perpendicular to the wind direction and the element.

b) Calculation of R_d for the Shaft Shaft
The total wind resistance in the direction of the wind over a panel height of the structural components of a lattice shaft of equivalent triangular cross section or square cross section having equal projected areas for each face may take as

$$R_d= k_\theta\, C_D\, A_f \quad (5)$$

Where:
k_θ=1.0+$k_1k_2 \sin^2 2\theta$ for square shafts
$k_\theta = 1.0$ equilateral triangular composed of circular member k_θ=1.0 - 0.1sin^{2}1.5θ Triangular composed of flat sided members
θ = is the angle of incidence of the wind to the face, in plan.
$k_1 = 0.55$ for shafts composed of flat sided member
$k_1 = 0.8$ for shafts composed of circular sided
$k_2 = 0.2$ $0.0 < \tau \leq 0.2$ and $0.8 < \tau \leq 1.0$
$k_2 = \tau$ $0.2 < \tau \leq 0.5$
$k_2 = 1 - \tau$ $0.5 < \tau \leq 0.8$
τ = is solidity ratio = ($A_{\text{exposed to wind}}$ / A_{total})
C_D = values of overall normal drag coefficients.
For such shafts composed of both flat sided and circular section members or for those composed entirely of circular sections appropriate to high Reynolds number, R_e .The overall normal drag (pressure) coefficient may be obtained from: -

$$C_D = (C_D)_F \frac{A_F}{A_T} + (C_D)_C \frac{A_C}{A_T} + (C_D)' \frac{A_C'}{A_T} \quad (6)$$

If $R_e \leq 4\text{x}10^5$

$$C_D = (C_D)_F \frac{A_F}{A_T} + (C_D)_C \frac{A_C}{A_T} \quad (7)$$

If $R_e \geq 4\text{x}10^5$

$$C_D = (C_D)_F \frac{A_F}{A_T} + (C_D)' \frac{A_C'}{A_T} \quad (8)$$

Where:

$$(C_D)_F = 1.76\, C_1(1- C_2\,\tau + \tau^2) \quad (9)$$

$$(C_D)_C = C_1(1-C_2\tau)+(C_1+0.875)\,\tau^2 \quad (10)$$

$$(C_D)' = 1.9-\sqrt{(1-\tau)(2.8-1.14C_1+\tau)} \quad (11)$$

$C_1 = 2.25$ for square towers
$C_1 = 1.9$ for triangular towers
$C_2 = 1.5$ for square towers
$C_2 = 1.4$ for triangular towers
A_F = area of flat parts
A_C = area of circular in sub critical regime
A_C' = area of circular in supercritical regime

6. The cases of study

Six cases are considered. these cases are:
a) Triangular tower with one level of cables with 10% initial tension.
b) Triangular tower with one level of cables with 20% initial tension.
c) Triangular tower with two level of cables with 10% initial tension.
d) Square tower with one level of cables with 10% initial tension.
e) Square tower with one level of cables with 20% initial tension.
f) Square tower with two level of cables with 10% initial tension.

For all these cases the important obtained results are drawn and tabulated in the following graphs and tables respectively.

7. Analysis and discussion

The horizontal displacement along the shaft for all study cases are shown in the following figures with list of figures given in the end of the paper.

7.1. Case (a)

It is noted that

1) The difference between the maximum displacement of three-dimension flexure element model and equivalent beam element model change from -6% to 15%.
2) The response of the model with lacing system IP=3 was greater than the model with lacing systems IP=2 and IP=1, however it is more stiff than other systems.
3) There was an increasing in the difference between the responses in the two models with change the lacing system. The lacing system (IP=1) had larger difference than others.
4) In smaller loads and S=0.6 the maximum horizontal displacement in three-dimension flexure element model was smaller than that one in equivalent beam element model for lacing system(IP=3).
5) There was an increasing in the difference between the responses in the two models with increasing in the spacing between legs. The model (S=1.2) had larger difference than others.
6) With increasing of load intensity, the difference in displacement increased.

With the following figures
The following symbols are used to define the mathematical model and its lacing.

IP=1 beam element model with lacing system 1
IP=2 beam element model with lacing system 2
IP=3 beam element model with lacing system 3
3D-IP=1 three dimensional model with lacing system 1
3D-IP=2 three dimensional model with lacing system 2
3D-IP=3 three dimensional model with lacing system 3
The chartsshow only wind intensity (U(10)) of 10,30and 60m/s.

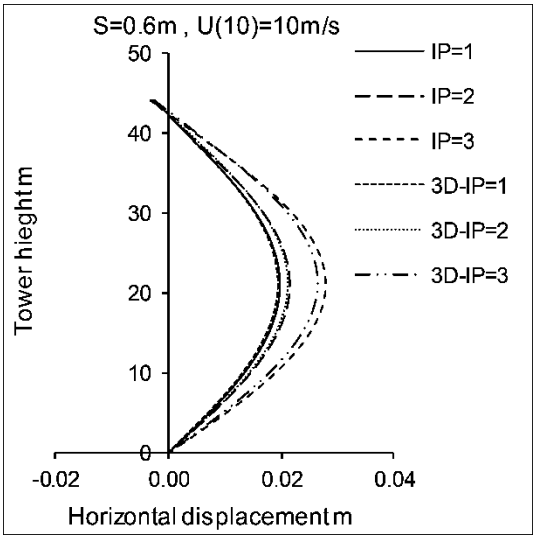

Figure 8: Variation of horizontal displacement along the shaft with change of mathematical model and lacing system and load intensity, S=0.6m,U(10)=10m/sec case (a).

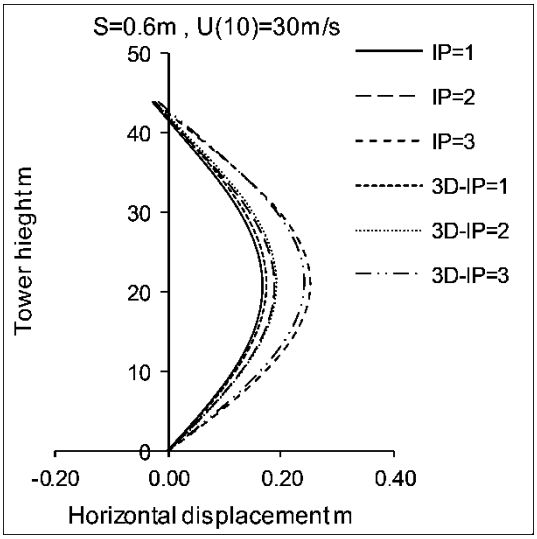

Figure 9: Variation of horizontal displacement along the shaft with change of mathematical model and lacing system and load intensity, S=0.6m, U(10)=30m/sec case (a).

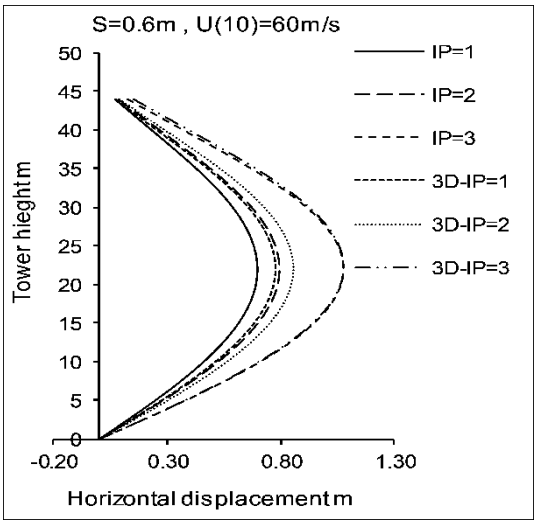

Figure 10: Variation of horizontal displacement along the shaft with change of mathematical model and lacing system and load intensity, S=0.6m, U(10)=60m/sec case (a).

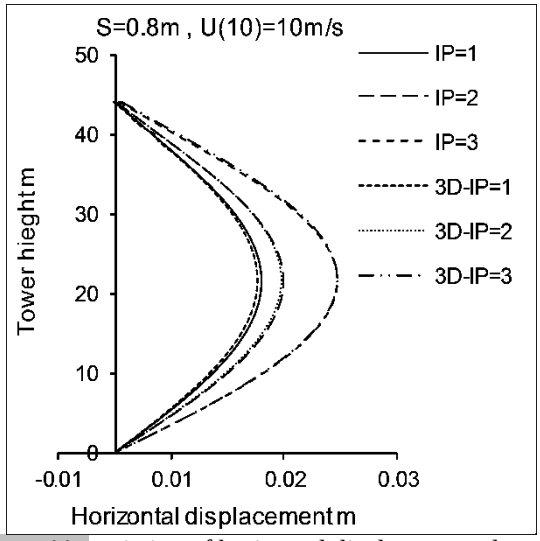

Figure 11: variation of horizontal displacement along the shaft with change of mathematical model and lacing system and load intensity, S=0.8m, U(10)=10m/sec case (a).

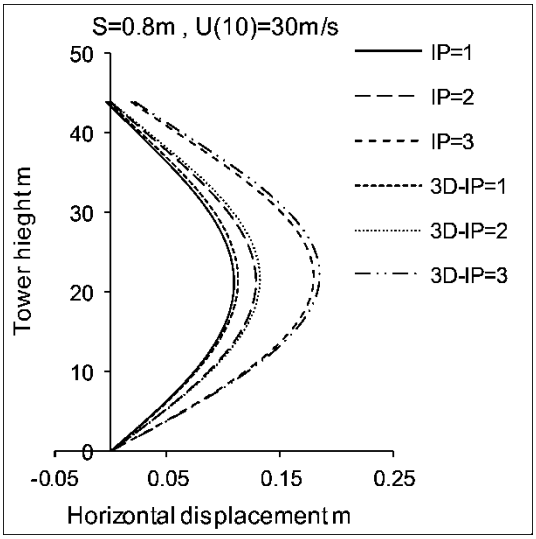

Figure 12: Variation of horizontal displacement along the shaft with change of mathematical model and lacing system and load intensity, S=0.8m, U(10)=30m/sec case (a).

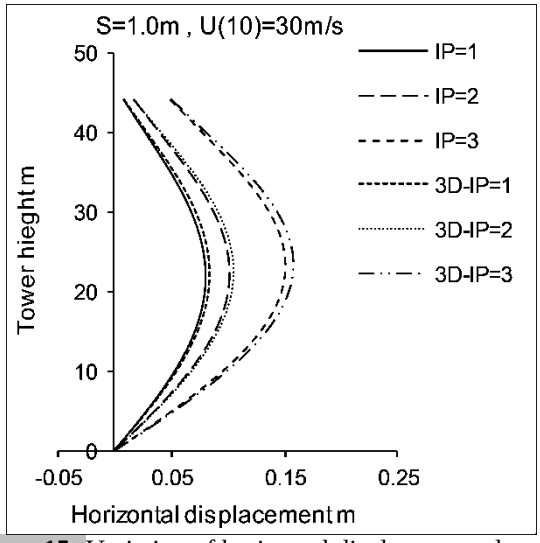

Figure 15: Variation of horizontal displacement along the shaft with change of mathematical model and lacing system and load intensity, S=1.0m, U(10)=30m/sec case (a).

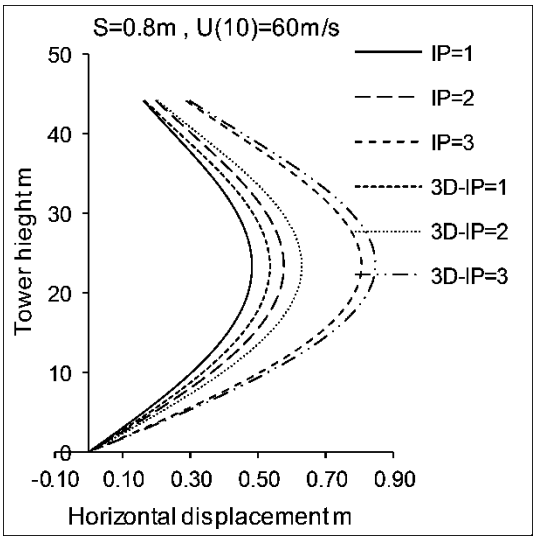

Figure 13: Variation of horizontal displacement along the shaft with change of mathematical model and lacing system and load intensity, S=0.8m, U(10)=60m/sec case (a).

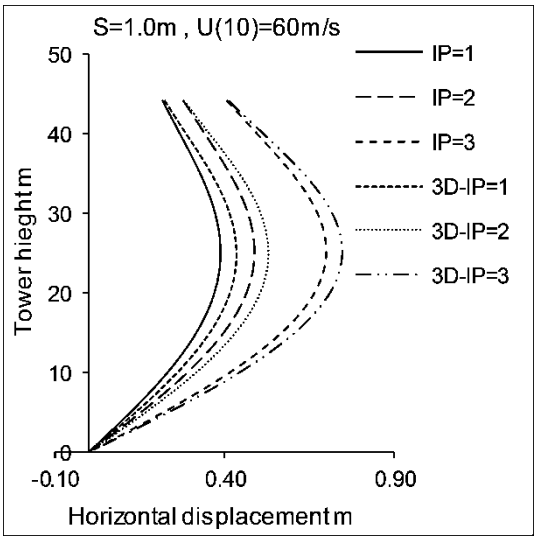

Figure 16: Variation of horizontal displacement along the shaft with change of mathematical model and lacing system and load intensity, S=1.0m, U(10)=60m/sec case (a).

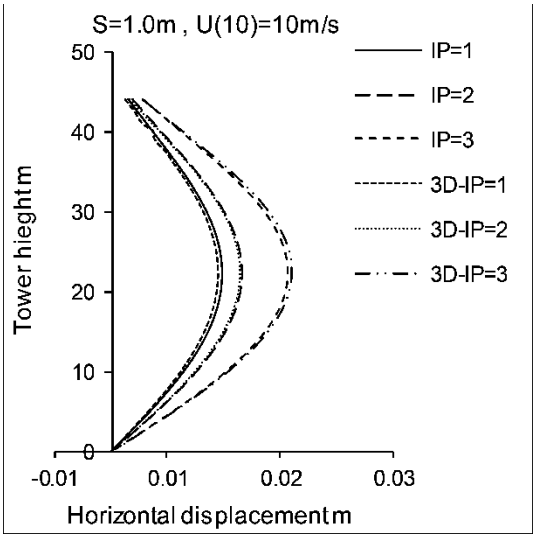

Figure 14: Variation of horizontal displacement along the shaft with change of mathematical model and lacing system and load intensity, S=1.0m, U(10)=10m/sec case (a).

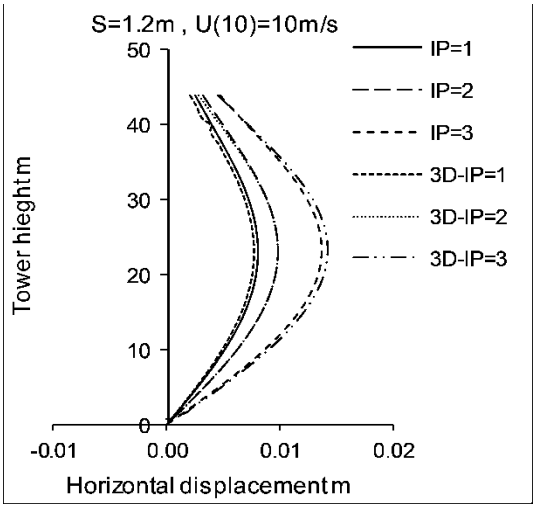

Figure 17: Variation of horizontal displacement along the shaft with change of mathematical model and lacing system and load intensity, S=1.2m, U(10)=10m/sec case (a).

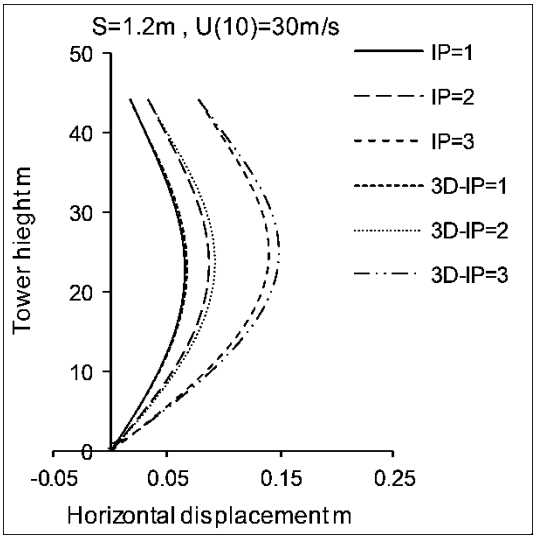

Figure 18: Variation of horizontal displacement along the shaft with change of mathematical model and lacing system and load intensity, S=1.2m, U(10)=30m/sec case (a).

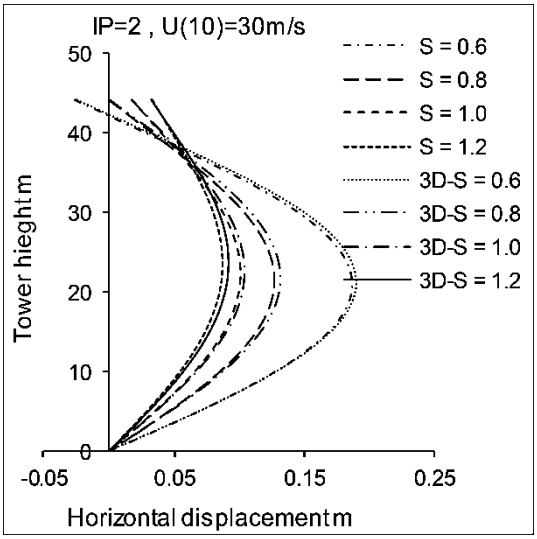

Figure 21: Variation of horizontal displacement along the shaft with change of mathematical model and spacing (S) with U(10)=30m/s for the lacing system IP=2 case (a).

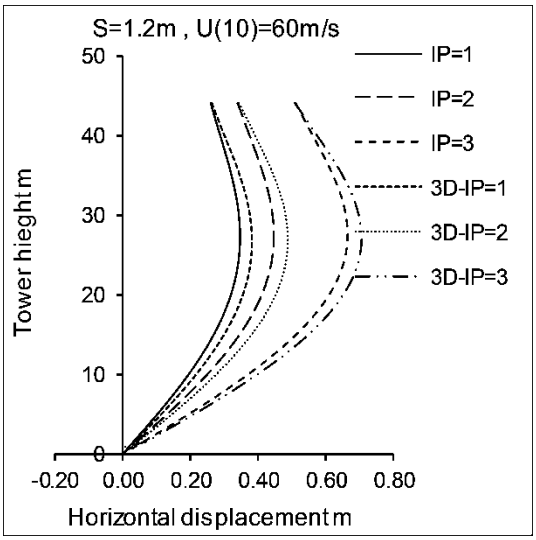

Figure 19: Variation of horizontal displacement along the shaft with change of mathematical model and lacing system and load intensity, S=1.2m, U(10)=60m/sec case (a).

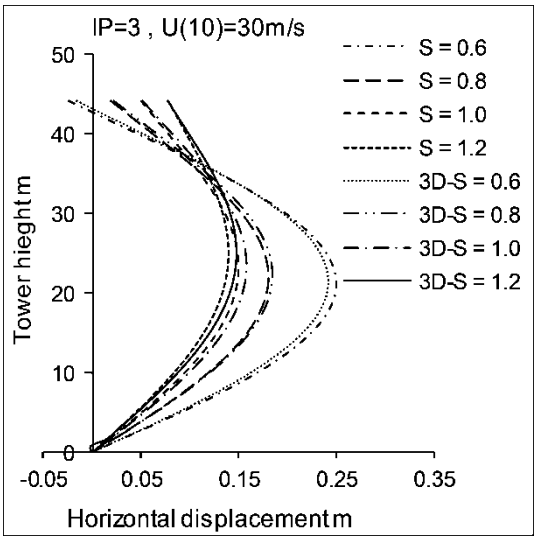

Figure 22: Variation of horizontal displacement along the shaft with change of mathematical model and spacing (S) with U(10)=30m/s for the lacing system IP=3 case (a).

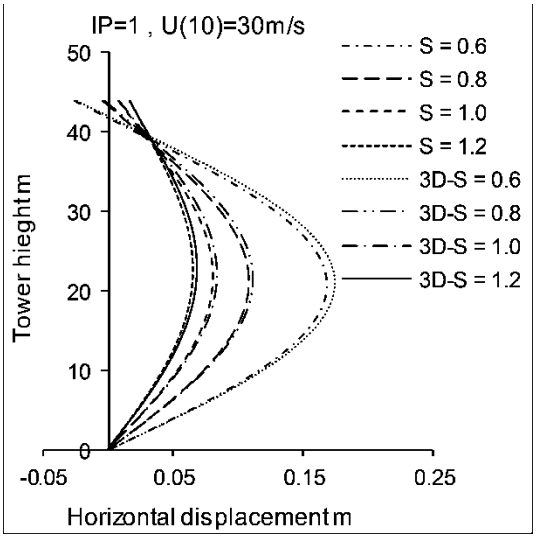

Figure 20: Variation of horizontal displacement along the shaft with change of mathematical model and spacing (S) with U(10)=30m/s for the lacing system IP=1 case (a).

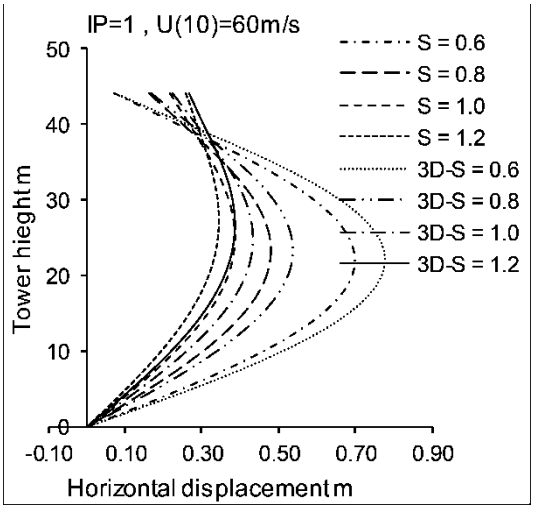

Figure 23: Variation of horizontal displacement along the shaft with change of mathematical model and spacing (S) with U(10)=60m/s for the lacing system IP=1 case (a).

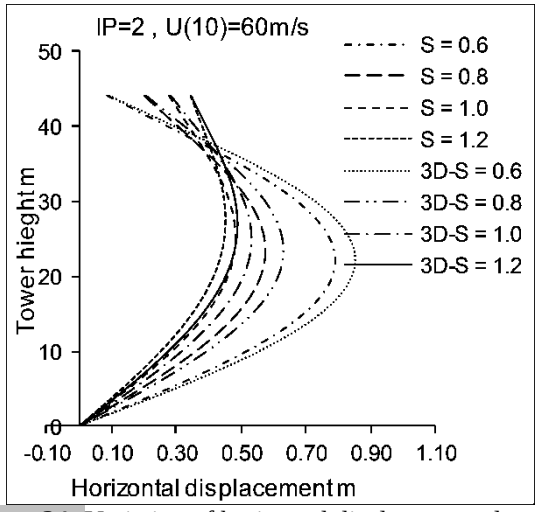

Figure 24: Variation of horizontal displacement along the shaft with change of mathematical model and spacing (S) with U(10)=60m/s for the lacing system IP=2 case (a).

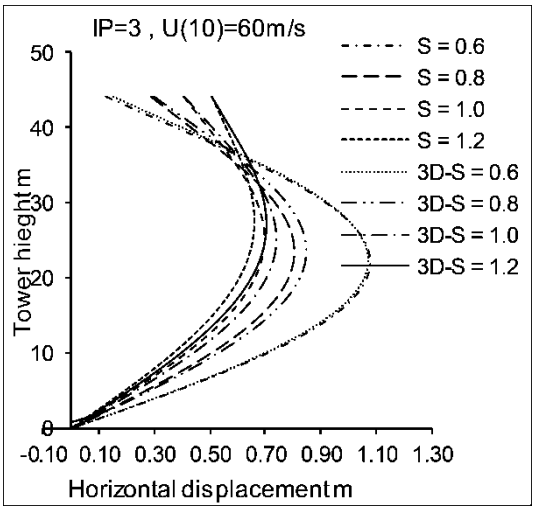

Figure 25: Variation of horizontal displacement along the shaft with change of mathematical model and spacing (S) with U(10)=60m/s for the lacing system IP=1 case (a).

For more clarification the following table showed the percentage of difference between maximum displacement in the three-dimension flexure element model to that one in the equivalent beam element model with all study parameters.

$$\text{Percentage}=\left(\frac{\text{max.displacement in 3D model}}{\text{max.displacement in eq. beam model}}-1\right)*100 \qquad (12)$$

Table 5: The referred percentage for case (a)

lacing system	space (m)	wind speed at height of 10 m U(10) (m/s)					
		10	20	30	40	50	60
IP=1	0.6	-1%	-1%	4%	13%	12%	11%
	0.8	-3%	-3%	3%	14%	12%	12%
	1	-4%	-5%	3%	14%	13%	12%
	1.2	-5%	-5%	4%	15%	12%	11%
IP=2	0.6	-2%	-2%	2%	8%	8%	7%
	0.8	-2%	-2%	3%	10%	9%	9%
	1	-2%	-2%	4%	11%	10%	9%
	1.2	-1%	-2%	4%	11%	9%	8%
IP=3	0.6	-5%	-5%	-3%	0%	0%	0%
	0.8	0%	0%	2%	5%	5%	5%
	1	2%	2%	5%	7%	7%	6%
	1.2	9%	10%	13%	14%	13%	12%

7.2. Case (b)

It is noted that
1) The same notes in the previous model
2) There was no effective change in deformation due to change of initial tension in low load intensity but the difference in displacement increasesin higher load intensity.

Table 6: The referred percentage for case (b)

lacing system	space (m)	wind speed at height of 10 m U(10) (m/s)					
		10	20	30	40	50	60
IP=1	0.6	-1%	-1%	4%	12%	12%	12%
	0.8	-3%	-3%	4%	14%	10%	9%
	1	-4%	-4%	4%	15%	15%	14%
	1.2	-5%	-6%	4%	15%	12%	11%
IP=2	0.6	-2%	-2%	2%	8%	8%	8%
	0.8	-1%	-1%	3%	11%	11%	10%
	1	-1%	-1%	5%	12%	12%	10%
	1.2	0%	-1%	6%	13%	12%	10%
IP=3	0.6	-5%	-5%	-3%	0%	0%	0%
	0.8	0%	0%	2%	6%	6%	5%
	1	2%	2%	5%	9%	8%	7%
	1.2	4%	4%	7%	10%	8%	8%

7.3 Case (C)

It is noted that
1. The same notes in the previous cases
2. The addition of level of cables decreased the deformation significantly.

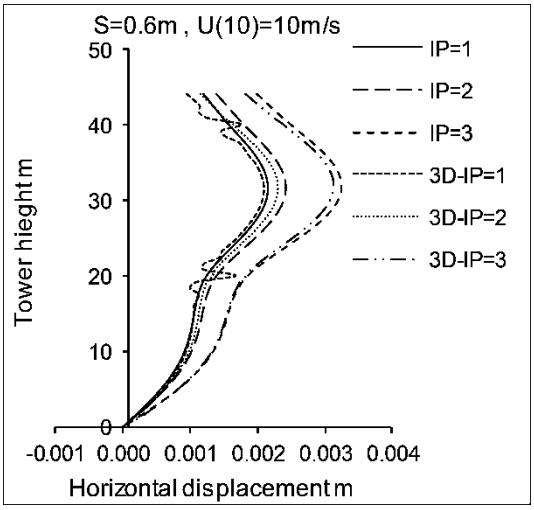

Figure 26: variation of horizontal displacement along the shaft with change of mathematical model and lacing system and load intensity, S=0.6m, U(10)=10m/sec case (c).

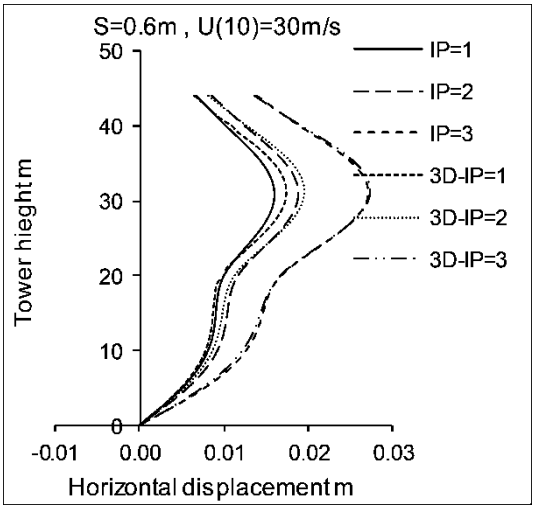

Figure 27: variation of horizontal displacement along the shaft with change of mathematical model and lacing system and load intensity, S=0.6m, U(10)=30m/sec case (c).

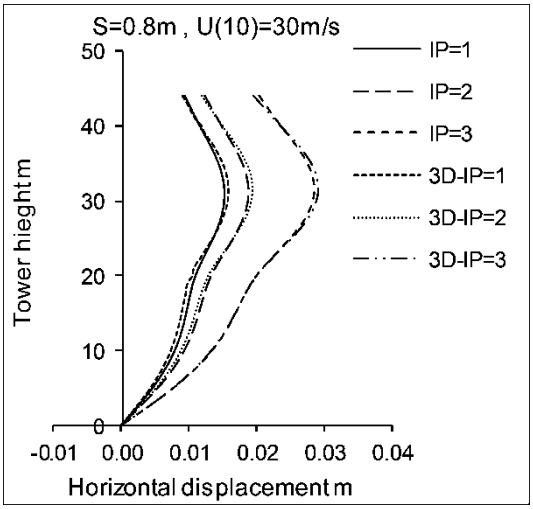

Figure 29: Variation of horizontal displacement along the shaft with change of mathematical model and lacing system and load intensity, S=0.8m, U(10)=30m/sec case (c).

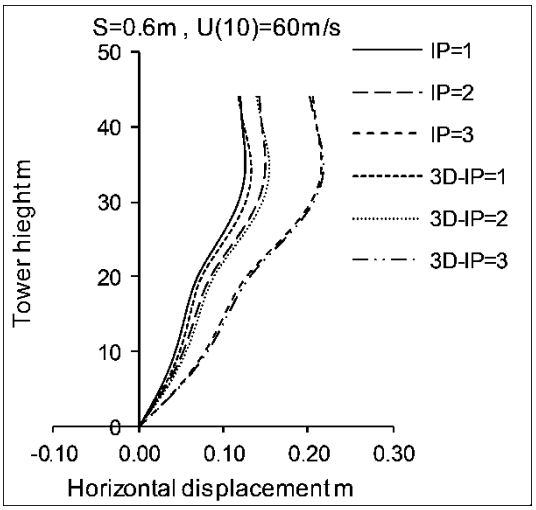

Figure 27: variation of horizontal displacement along the shaft with change of mathematical model and lacing system and load intensity, S=0.6m, U(10)=60m/sec case (c).

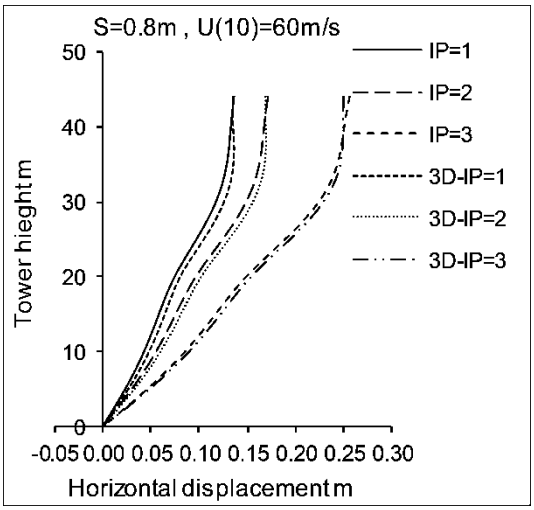

Figure 30: Variation of horizontal displacement along the shaft with change of mathematical model and lacing system and load intensity, S=0.8m, U(10)=60m/sec case (c).

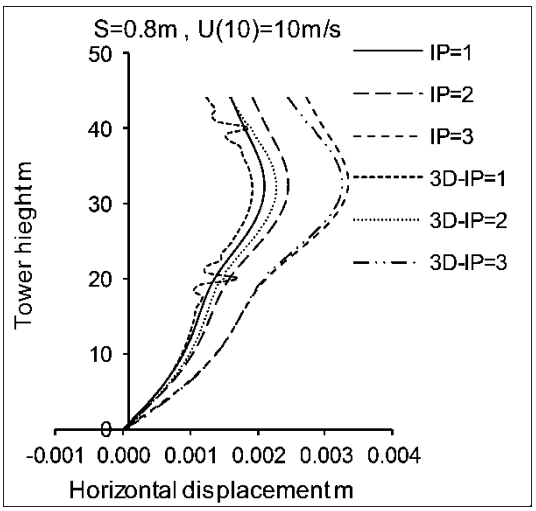

Figure 28: variation of horizontal displacement along the shaft with change of mathematical model and lacing system and load intensity, S=0.8m, U(10)=10m/sec case (c).

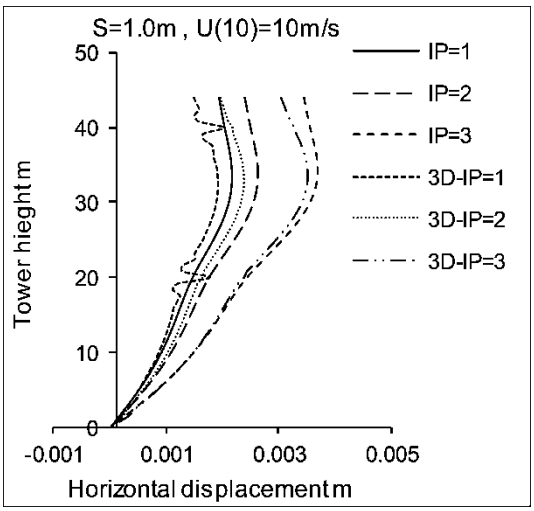

Figure 31: Variation of horizontal displacement along the shaft with change of mathematical model and lacing system and load intensity, S=1.0m, U(10)=10m/sec case (c).

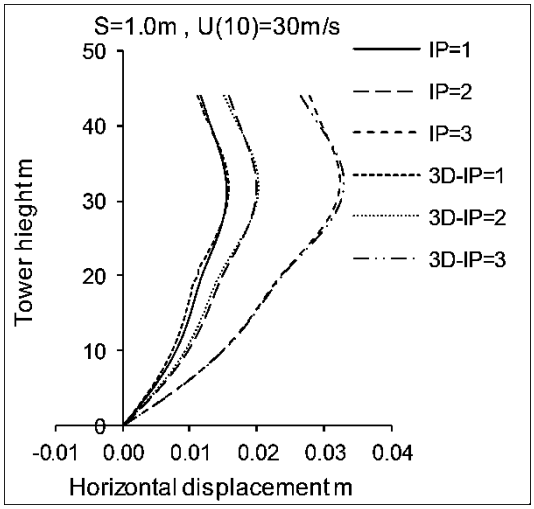

Figure 32: Variation of horizontal displacement along the shaft with change of mathematical model and lacing system and load intensity, S=1.0m, U(10)=30m/sec case (c).

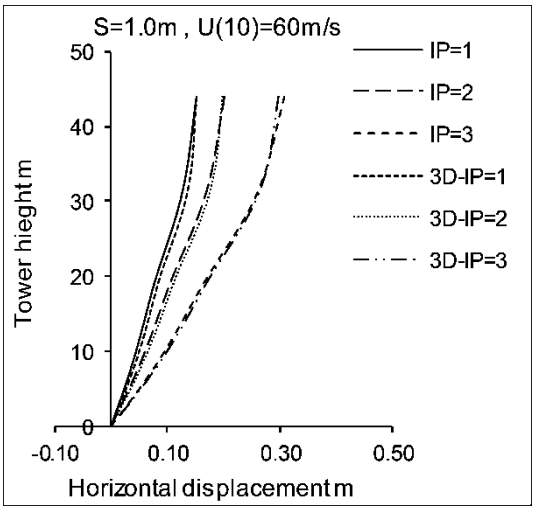

Figure 33: Variation of horizontal displacement along the shaft with change of mathematical model and lacing system and load intensity, S=1.0m, U(10)=60m/sec case (c).

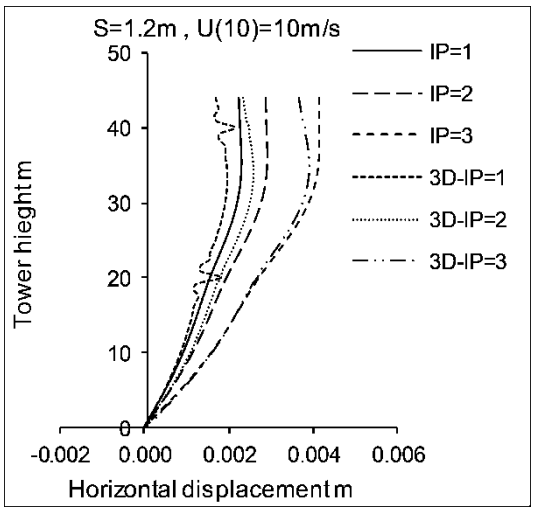

Figure 34: Variation of horizontal displacement along the shaft with change of mathematical model and lacing system and load intensity, S=1.2m, U(10)=10m/sec case (c).

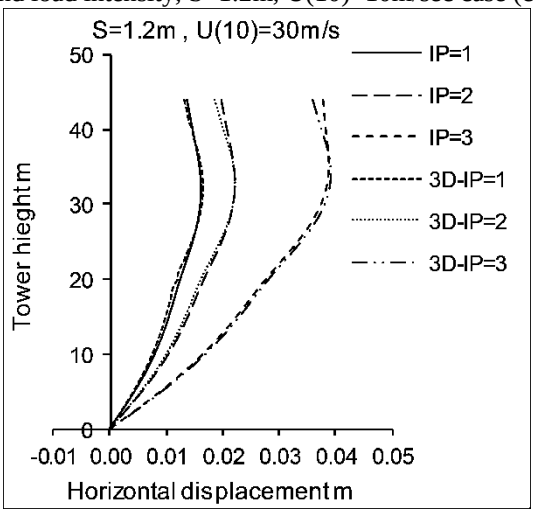

Figure 35: Variation of horizontal displacement along the shaft with change of mathematical model and lacing system and load intensity, S=1.2m, U(10)=30m/sec case (c).

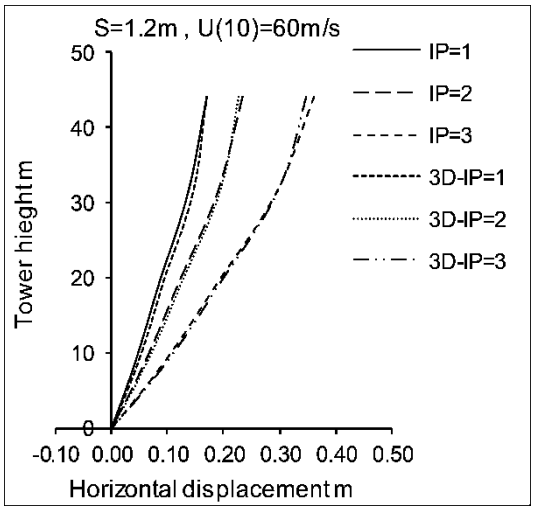

Figure 36: Variation of horizontal displacement along the shaft with change of mathematical model and lacing system and load intensity, S=1.2m, U(10)=60m/sec case (c).

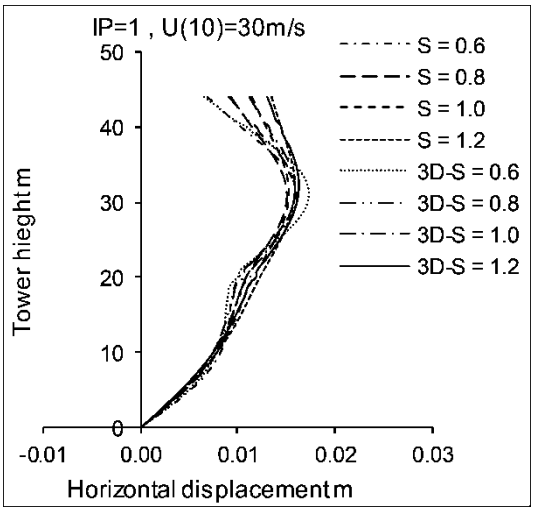

Figure 37: Variation of horizontal displacement along the shaft with change of mathematical model and spacing (S) with U(10)=30m/s for the lacing system IP=1 case (c).

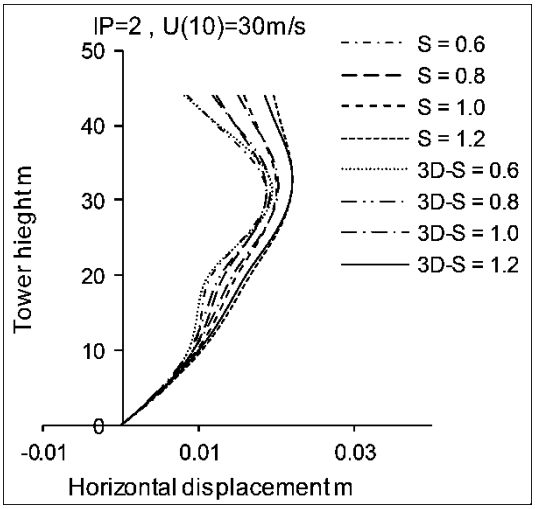

Figure 38: Variation of horizontal displacement along the shaft with change of mathematical model and spacing (S) with U(10)=30m/s for the lacing system IP=2 case (c).

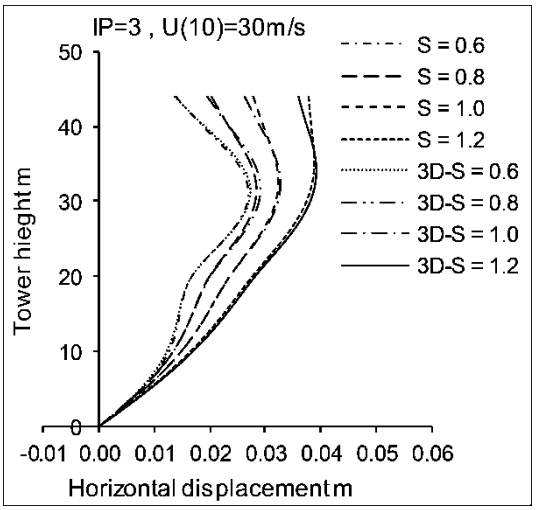

Figure 39: Variation of horizontal displacement along the shaft with change of mathematical model and spacing (S) with U(10)=30m/s for the lacing system IP=3 case (c).

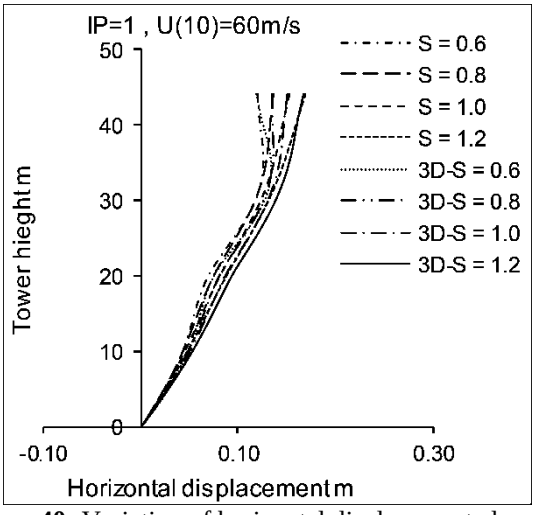

Figure 40: Variation of horizontal displacement along the shaft with change of mathematical model and spacing (S) with U(10)=60m/s for the lacing system IP=1 case (c).

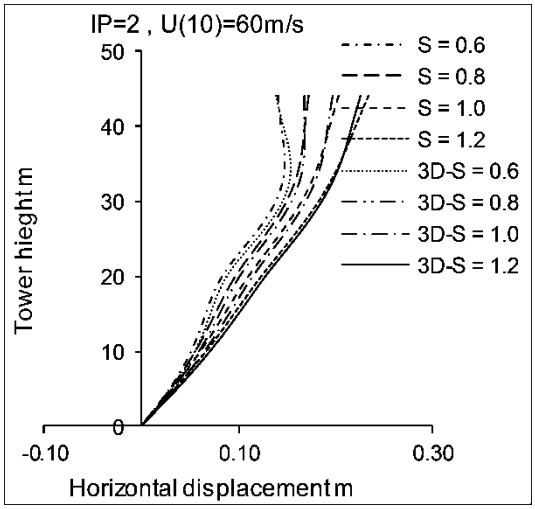

Figure 41: Variation of horizontal displacement along the shaft with change of mathematical model and spacing (S) with U(10)=60m/s for the lacing system IP=2 case (c).

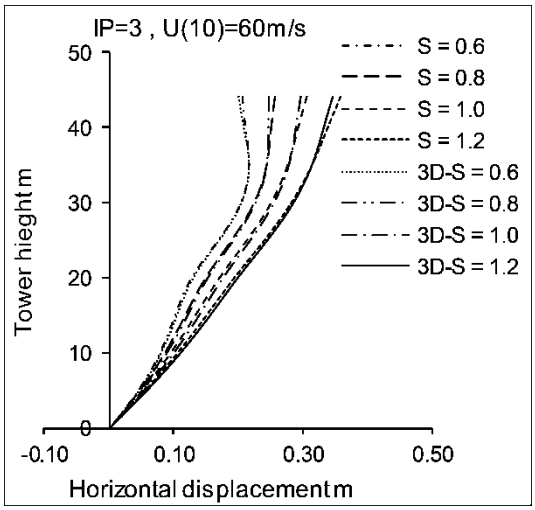

Figure 42: Variation of horizontal displacement along the shaft with change of mathematical model and spacing (S) with U(10)=60m/s for the lacing system IP=1 case (c).

Table 7: The referred percentage for case (c)

lacing system	space (m)	wind speed at height of 10 m U(10) (m/s)					
		10	20	30	40	50	60
IP=1	0.6	-4%	-5%	8%	11%	9%	6%
	0.8	-9%	-10%	6%	10%	6%	0%
	1	-8%	-13%	4%	9%	-1%	-1%
	1.2	-6%	-15%	3%	7%	-1%	-1%
IP=2	0.6	-5%	-6%	4%	6%	5%	3%
	0.8	-8%	-9%	3%	5%	1%	-2%
	1	-10%	-11%	1%	4%	-3%	-3%
	1.2	-12%	-12%	0%	-2%	-3%	-3%
IP=3	0.6	-3%	-4%	1%	2%	1%	1%
	0.8	-3%	-4%	2%	2%	-1%	-3%
	1	-4%	-5%	2%	-3%	-3%	-3%
	1.2	-5%	-6%	1%	-4%	-3%	-3%

7.4. Case (D)

It is noted that
The square section has some deference notes as flows:

1) The difference between the maximum displacement of three-dimension flexure element model and equivalent beam element model change from -1% to 20%.
2) The response of the model with lacing system IP=3 was greater than the model with lacing systems IP=2 and IP=1, however it is more stiff than other systems.
3) There was an increasing in the difference between the responses in the two models with change the lacing system. The lacing system (IP=1) had larger difference than others.
4) In S=0.6 the maximum horizontal displacement in three-dimension flexure element model was smaller than that one in equivalent beam element model for lacing system(IP=3).
5) There was an increasing in the difference between the responses in the two models with increasing in the spacing between legs. The model (S=1.2) had larger difference than others.

The following figure shows the variation of horizontal displacement along the shaft. The charts show only wind intensity (U(10)) of 30and 60m/s.

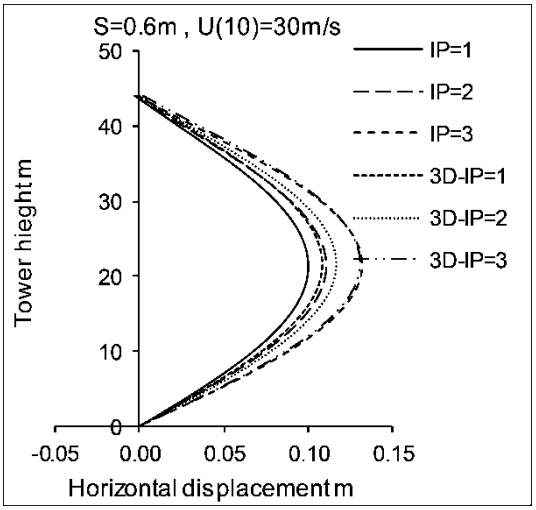

Figure 43: Variation of horizontal displacement along the shaft with change of mathematical model and lacing system and load intensity, S=0.6m, U(10)=30m/sec case (d).

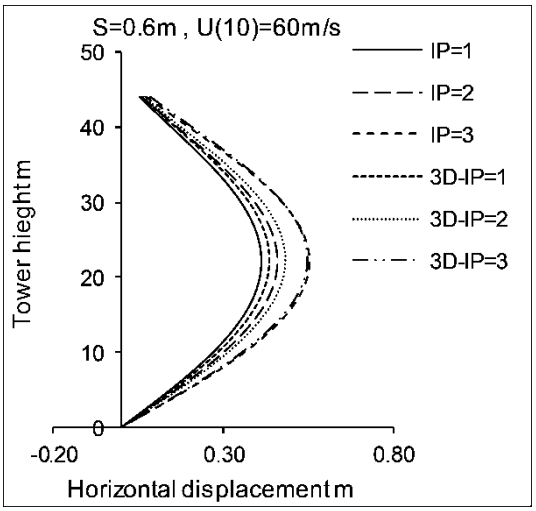

Figure 44: variation of horizontal displacement along the shaft with change of mathematical model and lacing system and load intensity, S=0.6m, U(10)=60m/sec case (d).

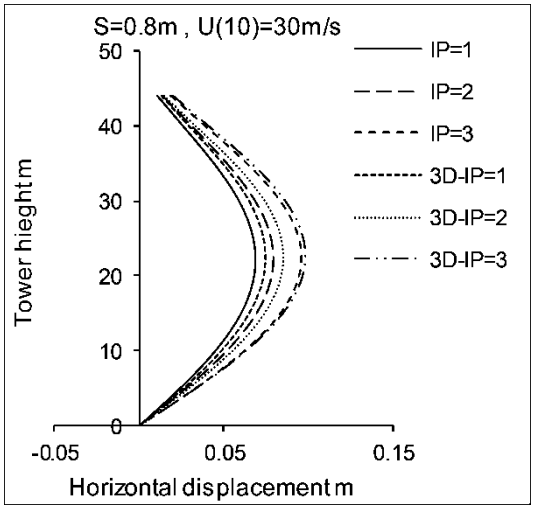

Figure 45: Variation of horizontal displacement along the shaft with change of mathematical model and lacing system and load intensity, S=0.8m, U(10)=30m/sec case (d).

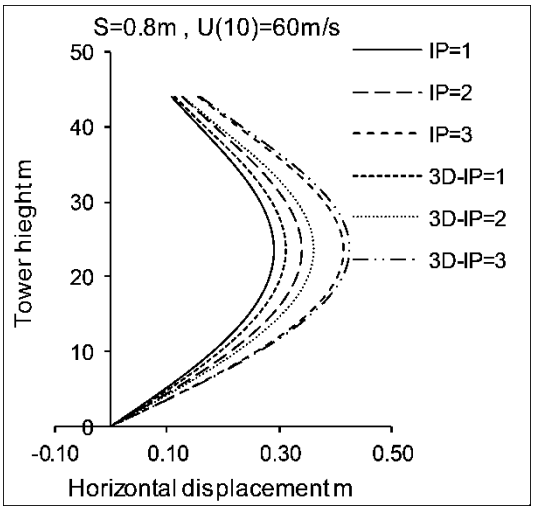

Figure 46: Variation of horizontal displacement along the shaft with change of mathematical model and lacing system and load intensity, S=0.8m, U(10)=60m/sec case (d).

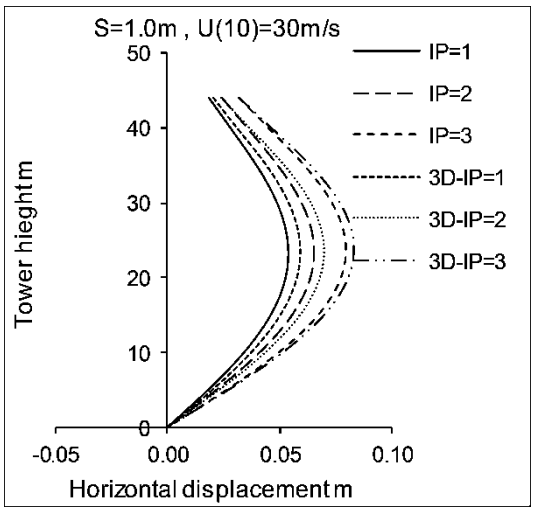

Figure 47: Variation of horizontal displacement along the shaft with change of mathematical model and lacing system and load intensity, S=1.0m, U(10)=30m/sec case (d).

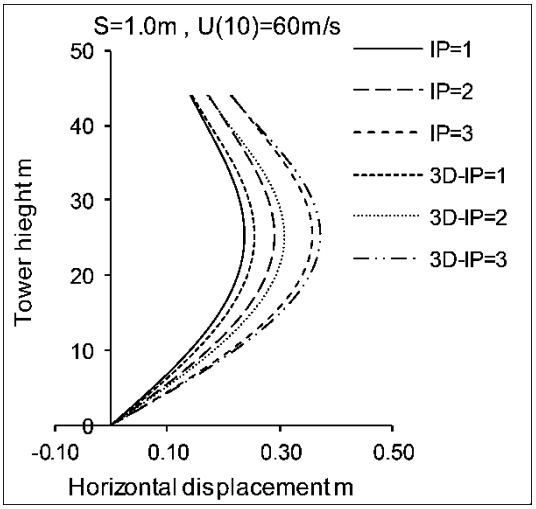

Figure 48: Variation of horizontal displacement along the shaft with change of mathematical model and lacing system and load intensity, S=1.0m, U(10)=60m/sec case (d).

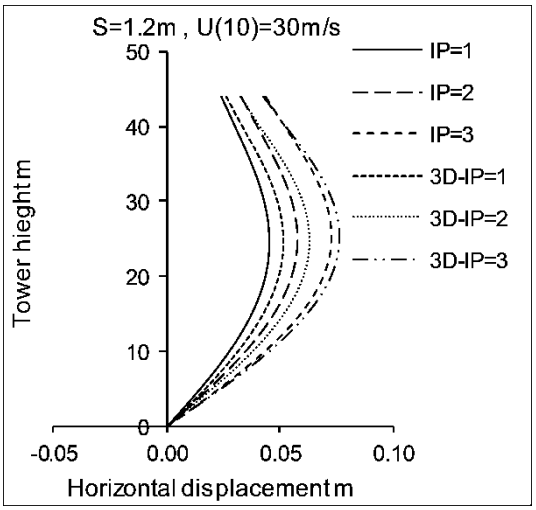

Figure 49: Variation of horizontal displacement along the shaft with change of mathematical model and lacing system and load intensity, S=1.2m, U(10)=30m/sec case (d).

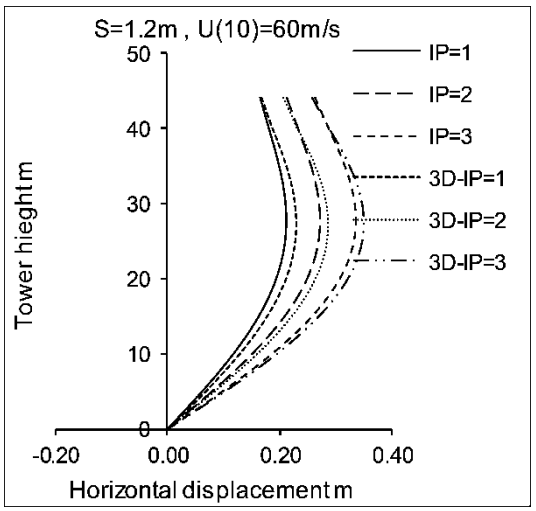

Figure 50: Variation of horizontal displacement along the shaft with change of mathematical model and lacing system and load intensity, S=1.2m, U(10)=60m/sec case (d).

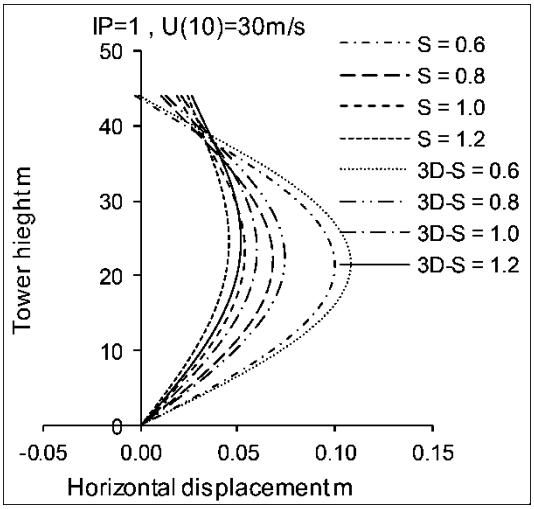

Figure 51: Variation of horizontal displacement along the shaft with change of mathematical model and spacing (S) with U(10)=30m/s for the lacing system IP=1 case (d).

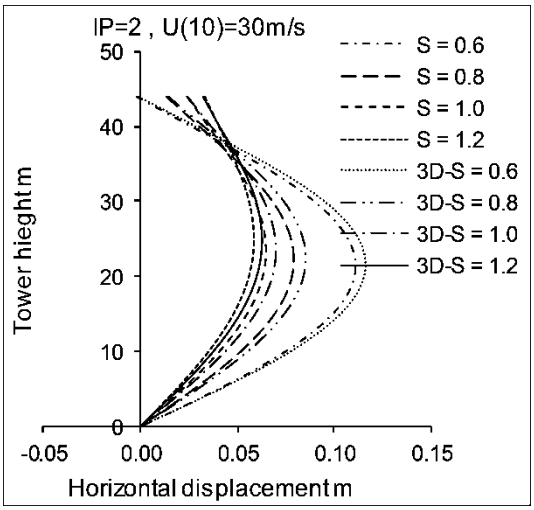

Figure 52: Variation of horizontal displacement along the shaft with change of mathematical model and spacing (S) with U(10)=30m/s for the lacing system IP=2 case (d).

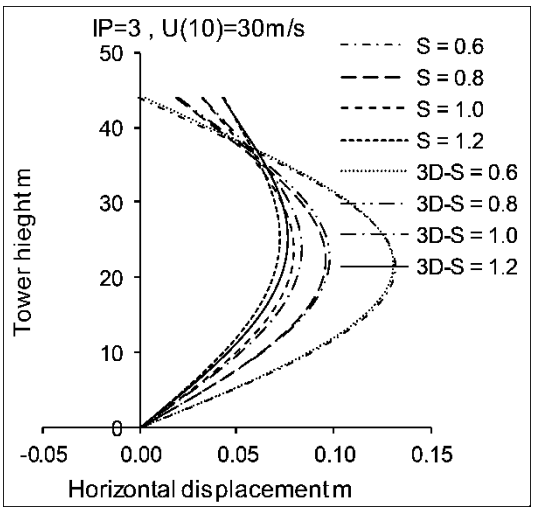

Figure 53: Variation of horizontal displacement along the shaft with change of mathematical model and spacing (S)with U(10)=30m/s for the lacing system IP=3 case (d).

Table 8: The referred percentage for case (d)

lacing system	space (m)	wind speed at height of 10 m U(10) (m/s)					
		10	20	30	40	50	60
IP=1	0.6	13%	9%	8%	7%	7%	7%
	0.8	14%	11%	10%	9%	8%	8%
	1	16%	13%	11%	10%	9%	9%
	1.2	18%	15%	12%	10%	9%	8%
IP=2	0.6	5%	5%	5%	4%	4%	4%
	0.8	8%	7%	7%	6%	6%	6%
	1	9%	8%	8%	7%	7%	6%
	1.2	10%	9%	8%	7%	6%	6%
IP=3	0.6	-1%	-1%	-1%	-1%	-1%	-1%
	0.8	3%	3%	3%	3%	2%	2%
	1	6%	5%	5%	4%	4%	4%
	1.2	7%	6%	5%	5%	4%	4%

7.5. Case (E)

It is noted that

1) The same notes in the previous model
2) There was no effective change in deformation due to change of initial tension in low load intensity but the difference in displacement increases in higher load intensity.

Table 9: The referred percentage for case (e)

lacing system	space (m)	wind speed at height of 10 m U(10) (m/s)					
		10	20	30	40	50	60
IP=1	0.6	14%	9%	8%	8%	7%	7%
	0.8	16%	12%	10%	10%	9%	9%
	1	18%	15%	12%	11%	10%	10%
	1.2	22%	17%	13%	12%	11%	10%
IP=2	0.6	5%	5%	5%	5%	5%	5%
	0.8	8%	7%	7%	7%	7%	6%
	1	10%	9%	9%	8%	8%	7%
	1.2	12%	10%	10%	9%	8%	7%
IP=3	0.6	-1%	-1%	-1%	-1%	-1%	-1%
	0.8	3%	3%	3%	3%	3%	3%
	1	6%	6%	6%	5%	5%	4%
	1.2	8%	7%	7%	7%	6%	5%

7.6. Case (F)

It is noted that

1) The same notes in the previous cases
2) The addition of level of cables decreased the deformation significantly.

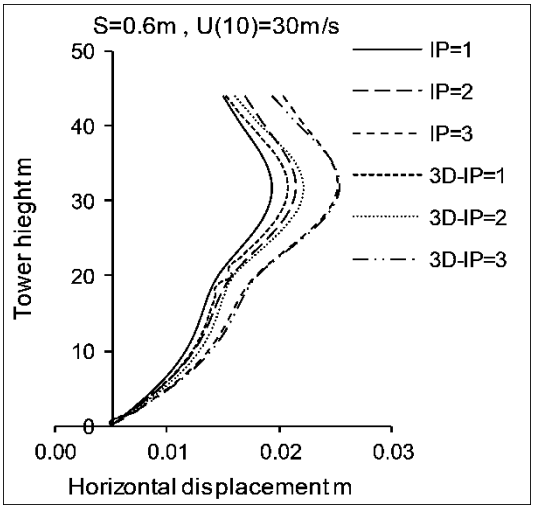

Figure 54: variation of horizontal displacement along the shaft with change of mathematical model and lacing system and load intensity, S=0.6m, U(10)=30m/sec case (f).

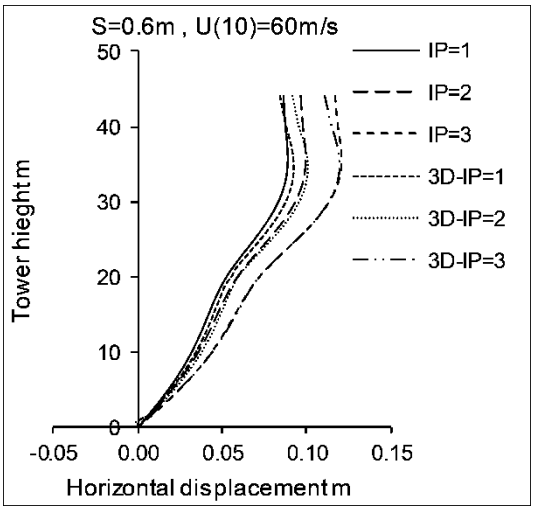

Figure 55: Variation of horizontal displacement along the shaft with change of mathematical model and lacing system and load intensity, S=0.6m, U(10)=60m/sec case (f).

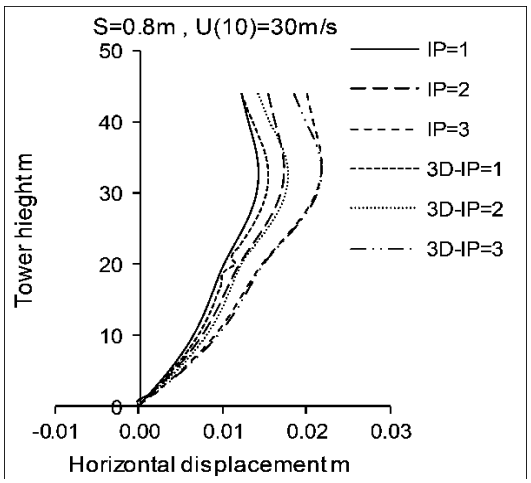

Figure 56: Variation of horizontal displacement along the shaft with change of mathematical model and lacing system and load intensity, S=0.8m, U(10)=30m/sec case (f).

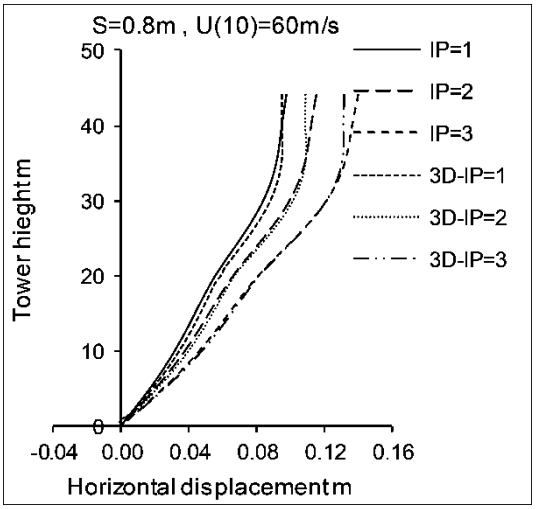

Figure 57: Variation of horizontal displacement along the shaft with change of mathematical model and lacing system and load intensity, S=0.8m, U(10)=60m/sec case (f).

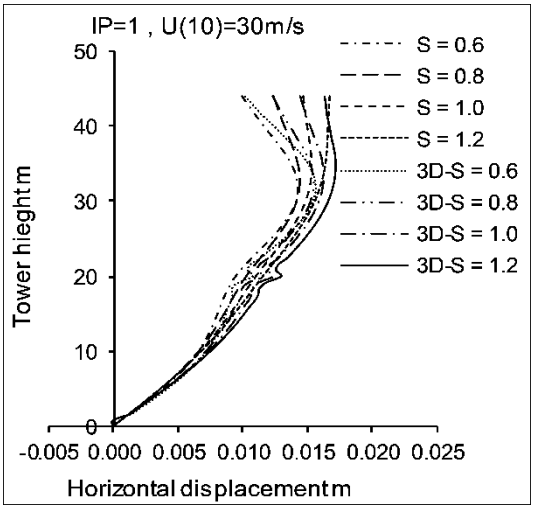

Figure 60: Variation of horizontal displacement along the shaft with change of mathematical model and spacing (S) with U(10)=30m/s for the lacing system IP=1 case (f).

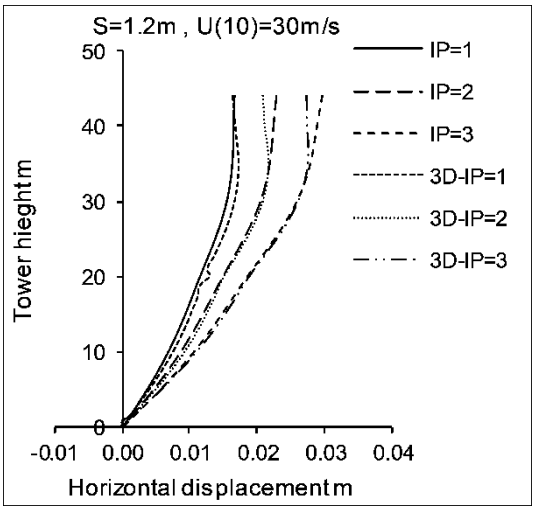

Figure 58: Variation of horizontal displacement along the shaft with change of mathematical model and lacing system and load intensity, S=1.2m, U(10)=30m/sec case (f).

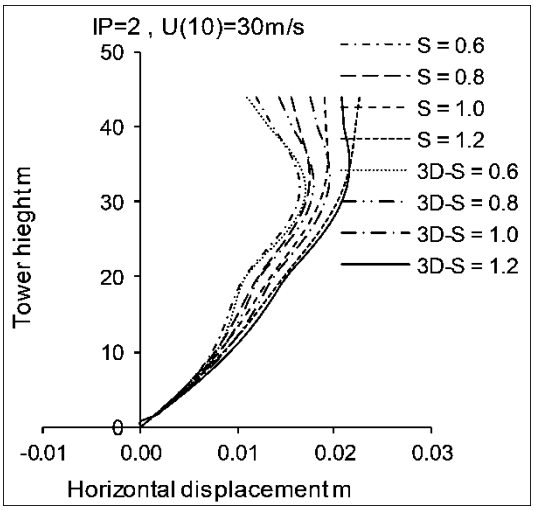

Figure 61: Variation of horizontal displacement along the shaft with change of mathematical model and spacing (S) with U(10)=30m/s for the lacing system IP=2 case (f).

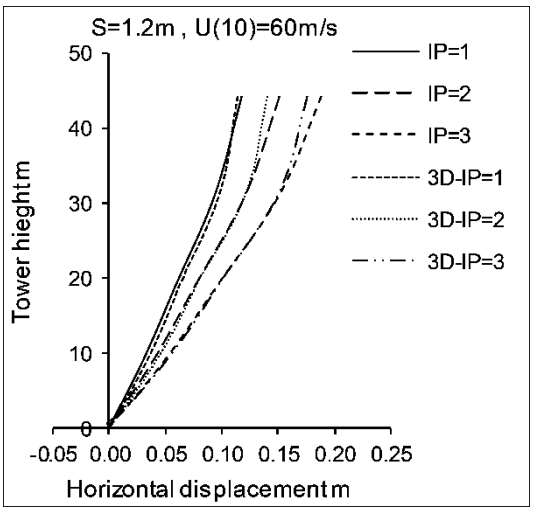

Figure 59: Variation of horizontal displacement along the shaft with change of mathematical model and lacing system and load intensity, S=1.2m, U(10)=60m/sec case (f).

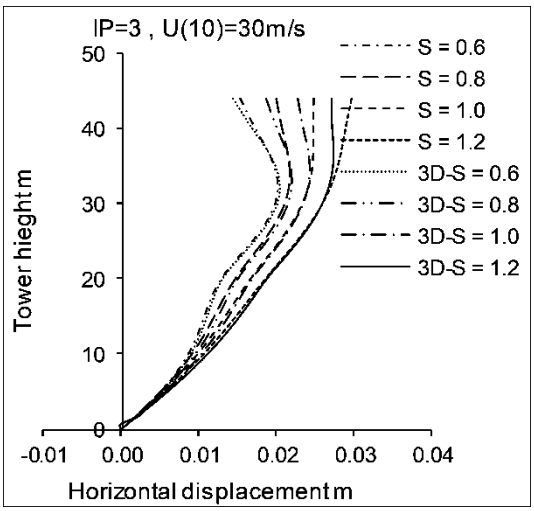

Figure 62: Variation of horizontal displacement along the shaft with change of mathematical model and spacing (S) with U(10)=30m/s for the lacing system IP=3 case (f).

Table 10: The referred percentage for case (f)

lacing system	space (m)	wind speed at height of 10 m U(10) (m/s)					
		10	20	30	40	50	60
IP=1	0.6	17%	13%	9%	-4%	5%	4%
	0.8	14%	11%	8%	-5%	0%	-3%
	1	13%	10%	6%	-13%	-4%	-4%
	1.2	10%	7%	2%	-19%	-4%	-4%
IP=2	0.6	7%	5%	4%	3%	2%	1%
	0.8	6%	4%	3%	0%	-4%	-6%
	1	4%	2%	0%	-7%	-7%	-6%
	1.2	2%	-2%	-5%	-8%	-7%	-7%
IP=3	0.6	2%	1%	1%	0%	0%	-1%
	0.8	3%	1%	0%	-1%	-5%	-6%
	1	2%	0%	-2%	-7%	-7%	-6%
	1.2	0%	-5%	-8%	-8%	-7%	-7%

8. Conclusions

8.1. Analysis of the shaft of guyed tower as equivalent beam element model gives deformation along the shaft with accuracy about (92) % of real deformation for triangular section and about (87) % of real deformation for square section

8.2. Increasing of lacing stiffness makes the model approaching to act as a one unite.

8.3. Increasing of space between legs leads to decrease of the stiffness of the three-dimension model.

8.4. The difference in displacement is shown clearly at higher value of load intensity.

8.5. The change of initial tensions has no effect on deformation in small deformation but it has small effect on deformation in larger load intensity.

8.6. The triangular section is better than square one as it acts approximately as one unit and has smaller loads from wind.

9. Acknowledgment

The authors wish to thank Mansoura University, Information Technology Institute in Cairo and the Egyptian Supreme Council of Universities for their technical and logistic support.

References

[1] ***, EN 1993-3-1:2006, Eurocode 3 – Design of steel structures – Part 3-1: Towers, shafts and chimneys.
[2] Pezo, M. L., et al.: Structural Analysis of Guyed Shaft Exposed to Wind Action THERMAL SCIENCE, Year 2016, Vol. 20, Suppl. 5, pp. S1473-S1483.
[3] Bazeos, N., et al., Static, Seismic and Stability Analyses of a Prototype Wind Turbine Steel Tower, Engineering Structures, 24 (2002), 8, pp. 1015-1025.
[4] Harikrishna, P., et al., Full Scale Measurements of the Structural Response of a 50 m Guyed Shaft under Wind Loading, Engineering Structures, 25 (2003), 7, pp. 859-867.
[5] Gioffre, M., et al., Removable Guyed Shaft for Mobile Phone Networks: Wind Load Modeling and Structural Response, Journal of Wind Engineering and Industrial Aerodynamics, 92 (2004), 6, pp. 463-475.
[6] Ben Kahla, N., Dynamic Analysis of Guyed Towers, Engineering Structures, 16 (1994), 4, pp. 293-301
[7] Ben Kahla, N., Nonlinear Dynamic Response of a Guyed Tower to a Sudden Guy Rupture, Engineering Structures, 19 (1997), 11, pp. 879-890
[8] Law, S. S., et al., Time-Varying Wind Load Identification from Structural Responses, Engineering Structures, 27 (2005), 10, pp. 1586-1598
[9] Wahba, Y. M. F., et al., Evaluation of Non-Linear Analysis of Guyed Antenna Towers, Computers and Structures, 68 (1998), 1, pp. 207-212.
[10] Saudi, G., Structural Assessment of a Guyed Shaft Through Measurement of Natural frequencies, Engineering Structures, 59 (2014), Feb., pp. 104-112.
[11] Battista, R. C. et al., Dynamic Behavior and Stability of Transmission Line Towers under Wind Forces, Journal of Wind Engineering and Industrial Aerodynamics, 91 (2003), 8, pp. 1051-1067.
[12] Yan-Li, H., et al., Nonlinear Discrete Analysis Method for Random Vibration of Guyed Shafts under Wind Load, Journal of Wind Engineering and Industrial Aerodynamics, 91 (2003), 4, pp. 513-525.
[13] da Silva, J. G. S., et al., Structural Assessment of Current Steel Design Models for Transmission and Telecommunication Towers, Journal of Constructional Steel Research, 61 (2005), 8, pp. 1108-1134.
[14] M. Naguib "Buckling Strength and Dynamic Response of Guyed Towers" Ph. D. Thesis, Mansoura University (1989).
[15] C. Gantes, R. Khoury, J. J. Connor and C. Pouangare " Modelling, Loading, and preliminary Design Consideration for tall guyed towers" Computers & Structures Vol. 49, No. 5, pp. 797-805, 1993.
[16] H. M. Irvine, Cable Structures. MIT Press (1981).
[17] Hobbs, R. E., Raoof, M., Behaviour of Cables under Dynamic or Repeated Loading, J. Construct. Steel Res., 39 (1996), 1, pp. 31-50.
[18] Desai, Y. M., Punde, S., Simple Model for Dynamic Analysis of Cable Supported Structures, Engineering Structures, 23 (2001), 3, pp. 271-279.
[19] Salehi, A. A. M., et al., Nonlinear Analysis of Cable Structures under General Loadings, Finite Elements in Analysis and Design, 73 (2013), Oct., pp. 11-19.
[20] Jayaraman, H. B., Knudsen, W. C., Curved Element for the Analysis of Cable Structures, Computers &Structures, 14 (1981), 3-4, pp. 325-333.
[21] J. W. Leonard, Tension Structures: Behavior and Analysis. McGraw-Hill (1988).
[22] Iass,"recommendation for the analysis and design of guyed shaft" London U. k. 1985.
[23] H.A. BUCHHOLDT "An Introduction to Cable Roof Structures", Cambridge University, Press, 1985.